

A correlation between moisture and compressive strength of a damaged 15-year-old rammed soil house

Adolfo Preciado^{*1}, Juan Carlos Santos^{1a}, Alejandro Ramírez-Gaytán^{2b},
Karla Ayala^{3c} and José de Jesús García^{4d}

¹Department of Habitat and Urban Development,
Western Institute of Technology and Higher Education (ITESO), 45604, Tlaquepaque, Jalisco, Mexico
²Department of Computational Sciences (CUCEI), University of Guadalajara (UdeG), 44430 Guadalajara, Jalisco, Mexico
³Department of Architecture, Technological Institute of Colima (ITC), 28979, Villa de Alvarez, Mexico
⁴Labconstru Maza, S.A. de C.V., 82134, Mazatlan, Sinaloa, Mexico

(Received March 5, 2020, Revised October 5, 2020, Accepted October 16, 2020)

Abstract. Earthen structures have an excellent bioclimatic performance, but they are vulnerable against earthquakes. In order to investigate the edification process and costs, a full-scale rammed soil house was constructed in 2004. In 2016-2019, it was studied its seismic damage, durability and degradation process. During 2004-2016, the house presented a relatively good seismic performance ($M_w=5.6-6.4$). The damaged cover contributed in the fast deterioration of walls. In 2018 it was observed a partial collapse of one wall due to recent seismicity ($M_w=5.6-6.1$). The 15-year-old samples presented a reduced compressive strength (0.040 MPa) and a minimum moisture (1.38%). It is estimated that the existing house has approximately a remaining 20% of compressive strength with a degradation of about 5.4% (0.0109 MPa) per year (considering a time frame of 15 years) if compared to the new soil samples (0.2028 MPa, 3.52% of moisture). This correlation between moisture and compressive strength degradation was compared with the study of new soil samples at the same construction site and compared against the extracted samples from the 15-year-old house. At 7-14-days, the specimens presented a similar compressive strength as the degraded ones, but different moisture. Conversely, the 60-days specimens shown almost five times more strength as the existing samples for a similar moisture. It was observed in new rammed soil that the lower the water content, the higher the compressive/shear strength.

Keywords: earthquakes; rammed soil; self-construction; decay; in-situ and laboratory testing; failure mechanisms; moisture content

1. Introduction

The use of soil to construct walls of adobe and rammed soil is a sustainable and a cost-effective option that has been implemented since the first generations that populated our planet. This natural material is characterized by its capability of durability that extends from centuries to thousands of years as shown in Fig. 1. In Fig. 1(a), it is illustrated a segment of the Great Chinese wall which was constructed in several periods of time since 221-770 BC to 1644-1911 of modern time. Preciado *et al.* (2017) affirm that several segments of the Great Chinese wall were constructed with an infill of rammed earth and covered with

carved stone for raining and defense protection. The needed construction tools were removable timber formworks and rammers of the same material. This technique was also applied in the infill of the Teotihuacan's pyramids in Mexico, which were constructed approximately in the year 250 of modern time (Fig. 1(b)). The great advantages of soil-based materials (i.e., combination of units and mortar in adobe or monolithic elements in rammed earth) for the construction of walls are their availability in almost every environment, bioclimatic properties (i.e., warm in winter and fresh in summer), self-build possibility without technical support or expensive tools, simplicity and rapidness in the construction. All these aspects have converted adobe and rammed soil into a very attractive construction material in different regions of the world, especially in Latin America (e.g., Peru, Colombia, Ecuador and Mexico). Adobe is a material made of rectangular units of sun-dried soil and placed together with mortar of the same material to mainly build walls. A typical enhancement technique (i.e., malleability increasing, excessive deformation prevention, rain protection and strength) was to add to the soil, natural materials such as cactus nectar, dried-grass, cattle's blood, manure, and in Peru, the hair of llama and alpaca. In Latin American countries is very common the use of adobe without plaster, as well as with

*Corresponding author, Professor, Ph.D.

E-mail: adolfopreciado@iteso.mx

^aMaster in Projects and Sustainable Constructions

E-mail: juancarlos_santos11@outlook.com

^bProfessor, Ph.D.

E-mail: l7m8s3r@gmail.com

^cArchitect

E-mail: aylab.karla11@hotmail.com

^dProfessor, Ph.D.

E-mail: labcon18@hotmail.com



(a) General view of the Great Chinese wall



(b) The Teotihuacan's pyramids in Mexico

Fig. 1 Historical buildings with an infill of rammed soil

(a) Adobe walls with plaster and typical color paint in Mexico (Preciado *et al.* 2015a)

(b) Combined adobe walls in Peru (Preciado and Santos 2019)

Fig. 2 Typical earthen housing of adobe

plaster and decorative color paint (Fig. 2(a)) and combinations (Fig. 2(b)).

In Mexico, it is very common to find adobe constructions of mainly one story with a double height of walls as shown in Fig. 2(a), meanwhile in Peru of two stories with a floor system of timber as illustrated in Fig. 2(b).

The roof system is usually constructed with the use of timber and compressed cardboard sheeting, or most of the time with fired-clay tiling as shown in Fig. 2. The great disadvantage of earthen walls such as adobe in Latin America, is that most of these zones are earthquake (EQ) prone areas with a high seismic risk due to the proximity of potential seismic sources and the presence of vulnerable auto-constructed houses (see Fig. 2). Most of these earthen houses are constructed without technical supervision and with combinations of materials such as debris from collapsed constructions in past EQs. These houses are very vulnerable against EQs of intermediate to high intensities due to the heavy weight of the soil, non-tensile strength of the material which induces a lack of structural integrity among perpendicular and parallel walls, as well as the strength degradation through time by aging and weathering.

However, soil-based walls are cost-effective and sustainable possibilities against conventional materials that deserve to be investigated more in detail to understand the

main components that convert them into highly vulnerable in terms of behavior and failure mechanisms under different loading conditions (i.e., axial and shear loading). The correct understanding of behavior and failure of this brittle material (e.g., Silva *et al.* 2014a, Taghiloha 2013, Morris *et al.* 2010, Islam and Watanabe 2004) is the key to identify different retrofitting strategies such as injected soil through shear cracks, meshes of natural/synthetic fibers (e.g., Bakir *et al.* 2017) or mixed with the soil matrix, and the stabilization with gypsum, ashes, clay or Portland cement (e.g., Islam 2002, Burroughs 2008, Silva *et al.* 2014b, Varum *et al.* 2014, Gupta and Kumar 2017, Yilmaz *et al.* 2018, Kim *et al.* 2018).

The main goal of the present paper is to investigate the uniaxial compression strength, shear resistance, decay and EQ performance of auto-constructed rammed soil houses in high seismic areas without maintenance as most of existing housing of this material. For this purpose, one existing rammed soil house constructed fifteen years ago (2004) for research purposes in one of the highest seismic areas of Mexico (Colima City) serves as a study subject. The compacted-soil house was self-build as a first instance to investigate the construction technique (i.e., foundation, walls, cover system and anchoring of timber elements), composite materials, geometry and the costs involved. Due to the heavy degradation state of the rammed soil house, in

summer 2018, it was decided to subject some parts of the building to destructive tests by the sampling extraction at walls to be tested in laboratory. The laboratory tests are aimed at correlating the compressive strength with the optimal water (or moisture) content of existing walls and approximately 20 new soil samples at different ages. The new soil samples were extracted at the construction site of the house to compare the behavior and failure modes of different specimens and wallettes with variation in age and water content under uniaxial compression and shear tests with those of the degraded existing construction. The optimal characteristics of the selected soil are determined by granulometry tests in laboratory and by qualitative/quantitative terms by suitable approaches used in geotechnics and highway engineering. Moreover, the water content is correlated with the compressive strength and aging of the existing rammed soil samples and with the new soil specimens at different ages (i.e., 7, 14, 45 and 60 days respectively).

2. Construction techniques, vulnerability aspects and mechanical properties of unstabilized rammed soil constructions

This section is aimed at describing the construction technique, main mechanical properties of unstabilized rammed soil walls and vulnerability aspects determining its performance and failure modes under static vertical loading and EQ induced lateral loading. The construction of rammed soil walls is relatively simple and one of the oldest techniques that has been used in many parts of the world due to the availability of this material and the lack of need for specialized constructors. The needed tools for its construction (i.e., formwork and rammer) are also simple and are made of timber and iron pipes. The formwork serves to pour the humid soil mix combined with dried straw (in some cases with other natural extracts and cattle manure) and the rammer serves for compaction by soil densification which is induced by the applied stress and displaced air from the pores. This process leads to the formation of solid load-bearing or architectonic walls to define spaces in an edification. The thickness of compacted soil walls mainly ranges between 30 to 60 cm depending on the total height of the wall, slenderness (i.e., aspect ratio), edification use, slabs and roof system, number of storeys and transmission of vertical loading. In order to construct the walls, the soil mix is poured into the formwork and compacted with the rammer in layers of about one third of the mold's height and when finished the three layers, the formwork is then located to form the following macroblock (see Section 4). Regarding the optimal characteristics of the soil mix for rammed soil purposes, it is recommended a combination of silt/clay, sand and gravel with the sufficient water content allowing to form a plastic mass. The plasticity of the soil mix may be tested by qualitative (e.g., by dropping a soil ball of 3 cm from a height of 1.5 m to the ground, e.g., Morel *et al.* 2001, Walker 2005, Preciado *et al.* 2017) and quantitative methods (e.g., particle size distribution by sieving and sedimentation, Keable 1994, 1996). Maniatidis and Walker (2003) affirm that several mixes have followed a 30-70% balance between clay/silt

and sand proportions (e.g., Dayton 1991, Easton 1996). De Morsier (2011) proposes the following ranges of granulometry in order to achieve an ideal soil-mix: 10-40% clay/silt; 35-65% sand and very fine gravel. Burroughs (2008) recommends typical values of about 25% clay, 60% sand and 15% gravel. Khadka and Shakya (2016) studied several rammed soil specimens with a 47.8% clay, 20.4% silt and 32% sand, and Maniatidis and Walker (2008) 12% clay, 13% silt, 45% sand and 30% gravel with a liquid limit of 49%, a plastic limit of 25% and a plasticity index of 24%. These limits of Atterberg (i.e., liquid, plastic and plasticity) are helpful to classify a soil in terms of water content and granulometry, so, if a certain soil has a liquid limit lower than 50% should be considered as a soil with a low plasticity index.

The optimum moisture (i.e., water) content of rammed soils is critical in order to achieve a maximum dry density through dynamic compaction, which is thought to be indexed to the strength and durability of the material (Taghiloha 2013). Moreover, Hall and Djerbib (2004) affirm that according to the Standards New Zealand (1998), the water content should never be below the 3% of the optimal water content, or 5% above it. De Morsier (2011) concludes that it is still unclear the impact on the physical, strength and durability characteristics of rammed soils induced by the variation of grading. Regarding the relationship between moisture and dry density, Burroughs (2008) found that the optimal water content for a soil mix ranges between 9.5 and 11%, resulting in a density of about 20 kN/m³ (2000 kg/m³). Bahar *et al.* (2004) also recommend a water content ranging from 9.5 and 11% for a compacted soil. Khadka and Shakya (2016) obtained an 8-10% of moisture content of the total mix by developing a dropping test to determine the soil's plasticity and usability as rammed soil. Hall and Djerbib (2004) used a value between 7 and 9% of moisture in relation to the soil mass for each of the 10 rammed earth soils under study. Maniatidis and Walker (2003) affirm that the density depends on the soil type, moisture content and compaction stress, and it may vary from 1700 to 2200 kg/m³ according to several research works (e.g., Houben and Guillaud 2008, Adam and Jones, 1995, Standards Australia 2002). The aforementioned relationship in terms of water content and density may affect the most important mechanical properties of rammed soil, related to the compressive strength and the elasticity modulus E (see Table 1). The main mechanical property affecting the overall resistance of rammed soil is the tensile/shear strength, which ranges between 10-15% of the compressive strength and it is recommended in literature to be taken as zero for calculation purposes (see Table 1). Meli (1998) affirms that the volumetric weight of adobe and rammed soil is of about 1800 kg/m³ and the main mechanical properties such as the compressive strength is in the range of 2-5 kg/cm² (0.20-0.50 MPa) and shear strength of about 0.5 kg/cm² (0.05 MPa) (see Table 1). Standards New Zealand (1998) specifies that the rammed soil as a construction material should present a minimum unconfined compressive strength of 1.3 MPa. Conversely, Houben and Guillaud (2008), Maniatidis and Walker (2008) affirm that the

Table 1 Summary of mean physical and mechanical properties of unstabilized/natural rammed soil specimens reported in literature

Reference	Density Ton/m ³	E MPa	σ_u MPa	τ_u MPa	ω_o %	ω_f %	Slenderness: samples in cm
Khadka and Shakya (2016)	1.95-2.35	N/M	1.5-3.1	N/M	8-10	N/M	1: (cubes 10x10x10)
Silva <i>et al.</i> (2014b)	1.83	340	1.26	0.15	13.4	N/M	2.75: (55x55x20)
Hall and Djerbib (2004)	2.05-2.16	N/M	0.75-1.46	N/M	7-9	N/M	1: (cubes 10x10x10)
Jaquin <i>et al.</i> (2006)	N/M	60	0.042-0.71	N/M	12	2-3	3.4: (102x99x30)
Maniatidis and Walker (2008)	1.85	160	2.46	N/M	12.5	N/M	2: (d=10, h=20)
Maniatidis and Walker (2008)	1.85	130	1.9	N/M	12	N/M	2: (d=30, h=60)
Maniatidis and Walker (2008)	1.76-2.03	60-70	0.62-0.97	N/M	10.5	5.1-7	2: (30x30x60)
Afanador-Garcia <i>et al.</i> (2013)	1.72-2	42-74	0.17	0.022	13.2	3.32	2: (25x50x50)
Meli (1998)	1.8	294	0.20-0.50	0.05	N/M	N/M	N/M

E= elasticity modulus; N/M= Not measured; σ_u = ultimate compressive stress; τ_u = ultimate shear stress; ω_o = initial water content; ω_f = water content at test; d= diameter; h= height



(a) In-plane failure of rammed soil walls (Morris *et al.* 2010) (b) Cover collapse by out-of-plane failure of adobe walls (Varum *et al.* 2014)

Fig. 3 Typical observed seismic failure modes of earthen housing

compressive stress by vertical loading at the bottom part of walls in single-storey buildings is of approximately 0.1-0.3 MPa, while the overall compressive strength is of about 1 MPa. Compared to fired-clay brick masonry, the compressive strength of unstabilized soil and adobe walls is acceptable but still reduced (e.g., Islam 2002, Islam and Watanabe 2004, Varum *et al.* 2014, Caporale *et al.* 2015 and Preciado and Sperbeck 2019). Table 1 illustrates a summary of relevant research works related to the water content of rammed soil at both, the day of fabrication of samples and the testing day, as well as the main physical/mechanical properties under uniaxial compression and shear by laboratory testing.

The main aspects determining the durability of rammed soil houses are integrated in two main groups: i) weathering degradation and aging of the material (e.g., Hall and Djerbib 2004, Hall 2007, Bui *et al.* 2009) and ii) structural vulnerability under sustained vertical loading and seismic effects (e.g., Preciado *et al.* 2017, Preciado and Santos 2019). Regarding the first aspect, weathering damage may occur when the walls are directly constructed over the ground without a stone masonry foundation which extends to the footing (constructed of stone or brick masonry),

regularly to the first third of the wall as observed in Fig. 2. The saturated ground during the raining season may affect the building's base by the capillarity effect (induced moisture) which weakens the soil particles by erosion, raining water, solar radiation and wind. The length of the light cover wings (ranging between 0.50 and 1 m) is also very important in order to protect the walls from the direct effect of raining water and solar radiation. The aforementioned drawbacks of self-constructed rammed soil houses are fundamental in the aging and rapid degradation of the material, which is also increased by the lack of maintenance.

Regarding the structural vulnerability under vertical and seismic loading, it is worth to mention that compressed soil walls show an acceptable behavior under vertical loading induced by the use of the building and self-weight of structural elements. This is the opposite in case of seismically induced forces. The main drawback is the lack of structural integrity, which is generated by the low tensile strength of the material. The last induces cracking even when subjected to reduced horizontal vibration such as the generated by the environment (i.e., traffic and wind). The cracking is mainly presented at the corners between façades (i.e., frontal, posterior or lateral) and the contact with other

perpendicular walls with a vertical distribution of cracks along the structural element. The lack of integrity has more impact under seismic loading due to the fact that the shaking induces a detachment between elements and complex brittle failure mechanisms in-plane and out-of-plane that may end in a partial or global collapse of the building with human casualties (Fig. 3). The overall behavior of earthen structures (i.e., adobe and rammed soil) is mainly governed by the low tensile strength, which agrees with the observed behavior (i.e., quasi-brittle) in vulnerable unreinforced masonry structures (e.g., Lourenço and Pina-Henriques 2006, Milani 2011a, b, Preciado *et al.* 2015a, b, Preciado and Sperbeck 2019), but even more brittle due to its inefficient mechanical properties. These aspects have also an impact on the poor seismic performance of rammed soil housing, in addition to the heavy mass of this material, brittleness, erosion and lack of connectivity among walls. The seismic behavior and failure mechanisms of this material depend on the nonlinear behavior since low horizontal seismic loading, anisotropy of the material and pre-existing cracking/damage. Another effect that complicates the behavior and failure is the loading direction and the anisotropy of the material which may induce different cracking propagation on walls in the plane, out-of-plane and combinations due to the material characteristics, aspect ratio of walls, mass, vertical loading, openings and so on. The in-plane failure is mainly represented by diagonal shear cracks at walls (Fig. 3(a)) and at the perimeter of openings (e.g., windows or doors) and by vertical cracking at the intersection of walls as aforementioned by the lack of structural integrity.

Conversely, the out-of-plane mode may occur by the rapid formation of a horizontal crack at the wall's base, followed by a global collapse or roof failure into the interior part due to supports vibration by the induced perpendicular loading (Fig. 3(b)). The construction of earthen structures represents interesting benefits from the economical and sustainable point of view against conventional materials such as masonry and concrete that deserve to be investigated in detail from different approaches to understand the main components that determine its very high seismic vulnerability. This knowledge in behavior and failure under different loading conditions (i.e., uniaxial compression, shear, bending and so on) would allow to propose suitable retrofitting proposals able to avoid human casualties in case of intermediate to strong EQs. The study of this brittle material is a topic of great importance and very active research by the scientific community in terms of construction techniques, behavior and failure modes (e.g., Morris *et al.* 2010, Taghiloha 2013, Silva *et al.* 2014a, Preciado *et al.* 2017, Preciado and Santos 2019) to identify strengthening techniques with sustainable materials as soil injection, natural fibers and stabilization cements (e.g., Islam 2002, Burroughs 2008, Silva *et al.* 2014b, Varum *et al.* 2014). The stabilization of rammed soil increases its strength, durability and elastic properties as Young's modulus (e.g., Bahar *et al.* 2004).

3. Seismic context of Colima, Mexico

Mexico is located in the belt of fire, which is

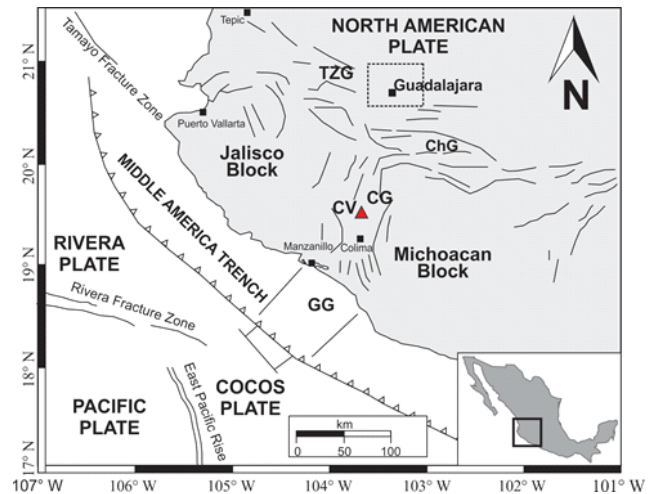


Fig. 4 Overview map of the tectonic environment of the Colima-Jalisco region and MZG (Flores-Estrella *et al.* 2018), adapted from (DeMets and Traylen 2000)

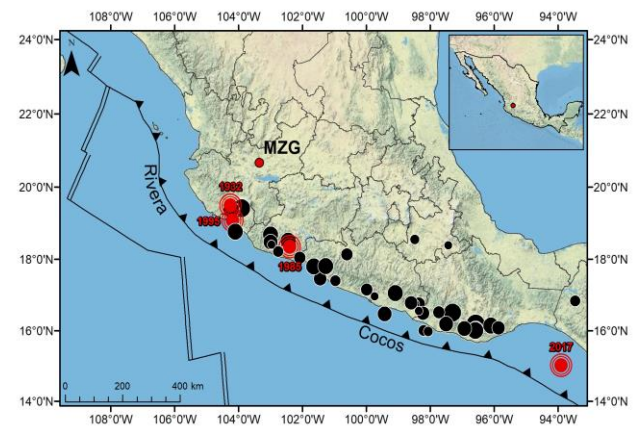


Fig. 5 Overview map of the seismological context of the Colima-Jalisco region where the red spots represent the most destructive EQs (Flores-Estrella *et al.* 2018)

Table 2 Summary of the main destructive EQs ($M_w > 7$) in the Colima-Jalisco region (SMIS and EERI 2006, Chavez *et al.* 2014)

Event	Date	Lat. N	Long. W	M_w	Intensity MMI in Colima	Fault system
1	06/03/1932	19.80°	104.00°	8.0	VIII	R and N.A.
2	06/18/1932	18.95°	104.42°	7.8	IX	Aftershock of 1
3	04/15/1941	18.85°	102.94°	7.6	X	C and N.A.
4	01/30/1973	18.39°	103.21°	7.6	VIII	C and N.A.
5	10/09/1995	18.79°	104.47°	8.0	VII	R and N.A.
6	01/21/2003	18.63°	104.13°	7.5	VIII	C and N.A.

Plates that generated the seismic event: R= Rivera; N.A.= North American and C= Cocos

characterized by the presence of very active volcanoes and high seismicity due to the interaction between plates with the large Pacific plate. At a national level, the seismic hazard is subdivided in four main zones (A-D), where A represents low seismicity and D a very high seismicity. The

state of Colima (see the black rectangle of Fig. 4 next to the port of Manzanillo at the Pacific coast) is located in the seismic zone D, which is classified as a very high seismic zone. Colima is the name of both, the state and the City, and adjoins to the state of Jalisco in the NE direction.

The great metropolis of Guadalajara (MZG) is also located in Jalisco (see Fig. 4 and the red spot in Fig. 5). The seismic hazard at this coastal region is mainly due to the interaction with the Pacific plate and three other main plates such as the Cocos, Rivera and North American. Most of the time, the rupture mechanism is mainly due by the subduction of either the Cocos or Rivera plate beneath the North American one, inducing destructive EQs approximately every eight to ten years as shown in Fig. 5 and Table 2. These seismic events have historically affected the region with magnitudes higher than $7M_w$ and intensities ranging from VII to X according to the modified Mercalli intensity (MMI) scale (e.g., Zobin *et al.* 2006 and Zobin and Pizano-Silva 2007).

Bandy *et al.* (1995) affirm that another potential seismic source close to the state of Colima is the so-called Jalisco block (Fig. 4), which is mainly activated by the Rivera and North American plates. In this area have occurred small to moderate EQs with ground accelerations of approximately eight times higher than the recorded at the subduction zone (Fig. 4). As aforementioned, the Colima-Jalisco region is an EQ prone area under high risk. This risk is even increased by the location of vulnerable auto-constructed buildings of inadequately confined masonry and earthen materials (see Figs. 2 and 3). The overview map of Fig. 5 illustrates the most destructive EQs that have affected the Colima-Jalisco region, and are summarized in Table 2.

In Fig. 5, it is worth noting the most destructive events that caused thousands of deaths and multiple collapses in Mexico City (1985 $M_w=8.1$ and 2017 $M_w=7.1$). The 1985 seismic event occurred in front of the coastal area of Lázaro Cárdenas in the state of Michoacán, which adjoins to the states of Colima and Jalisco and is located more than 350 km away from Mexico City. The inadequate soil conditions at the historical Centre of Mexico City and the presence of vulnerable buildings exhibited brittle collapses by soil-structure interaction inducing more than 20,000 deaths and multiple damages in historical buildings (see Fig. 5 and Table 2). According to Ruiz-García (2017), the seismic amplification effects by soil-structure interaction (i.e., resonance effect) occurred once again in Mexico City on September 19th, 2017. In this case, the epicentre was located at the central part of Mexico next to Puebla and Morelos ($M_w=7.1$). It is worth noting that the epicenter shown in Fig. 5 corresponds to the first seismic event occurred on September 7th, 2017 ($M_w=8.2$) at the southern Pacific coast and was not as destructive as the second event on September 19th (Preciado *et al.* 2020a, b).

4. Construction process of the rammed soil house under study

This section is aimed at briefly presenting the construction process of the compressed soil house at a real scale under study which was constructed by following empirical rules and typical materials used in the region. The

rammed earth house was constructed in summer 2004 at the posterior part of the *Instituto Tecnológico de Colima* (ITC), Mexico (Figs. 6-8). The self-build earthen house has a square plan of 3.5 x 3.5 m (12.25 m²) with a constant wall thickness of 0.40 m (Fig. 6(a)) and a height of 1.90 m. The total height is of about 2.64 m including the cover system with a triangular timber roof (Fig. 6(b)). The overall dimensions (i.e., total height, plan, wall thickness and openings), architecture design and materials of the rammed soil house were selected by taking into account similar adobe houses in the region of Colima-Jalisco, Mexico. As explained in the previous section, the entire state and City of Colima are under a very high seismic hazard due to the proximity of potential EQ sources (i.e., subduction zone at the Pacific coast, active volcano and inland grabens). The soil to be used was taken from an existing excavation at about 15-20 m from the selected construction site of the house (Fig. 7(a)). The usability of the soil was determined by the qualitative method of the dropping soil ball to the ground from a height of about 1.5 m with an optimal moisture content of 12-17%, and the sample presented no cracks. This means that the soil contains a proper content of fines, sand and gravel with a sufficient plasticity to be used as a compacted soil. Furthermore, the soil was improved in terms of durability against cracking by contraction due to temperature changes and rain with the addition of dried straw segments ranging from 5 to 10 cm (see Fig. 7(c)). For the foundation it was excavated a ditch of about 50x50 cm (width x height) without stone masonry at the bottom or other stiff material (Fig. 7(a)). The addition of a stone foundation at the wall's foot would have been better to avoid humidity by capillarity. At that time, in 2004, the aim of constructing a rammed soil house was to study the construction process and the involved costs, and to demolish it in January 2005 due to the expansion of the ITC, that for luck, the house was out of the limits of the new buildings. The rammer and the removable formwork (0.40x0.50x0.93 m) were constructed with reused timber and other low-cost materials covered with used motor oil for a better contact with the humid soil to avoid sticking and fast demolding (Fig. 7(b)). The wooden formwork has frontal/back openings for the construction of corner segments, overlapping and different alignment patterns of the soil macroblocks as shown in Fig. 7(d). The addition of open sides in the formwork along the width of the wall prevents the formation of distinct vertical joints which may induce the vertical crack initiation in case of closed sides. The macroblocks (see Fig. 8) followed an organized pattern to form monolithic elements able to transmit the vertical loading induced by its self-weight and roof system to the ground.

A set of steel wires were anchored at the wall's corner by the use of a timber segment of 20x40 cm from the bottom to the top part of walls and anchored at the perimeter beam (at 2 m height) for confining purposes (Fig. 8a). The authors of this paper consider that the addition of steel wires was not the best technique due to the incompatibility of deformations and corrosion problems. For instance, it would be more effective the use of timber poles at the four corners and openings, or the confining of the complete wall segments instead of only at the corners

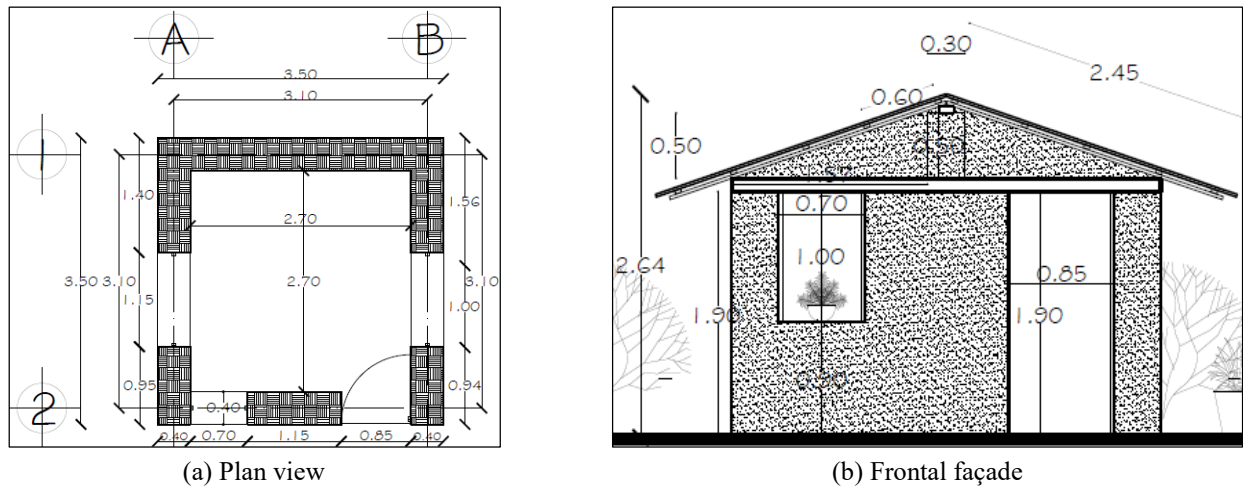


Fig. 6 Constructed rammed soil house at a real scale in 2004 for research purposes (metres)



(a) Ditch excavation for the wall's foundation



(b) Wooden mold and rammer



(c) Soil mix with dried straw



(d) General view of the removable formwork and macroblocks

Fig. 7 Initial construction process of the rammed soil walls

with the steel wires. Fig. 8(b) illustrates the soil mix pouring and compaction process to reach the final wall's height of 1.90m, as well as the usability of the scalable formwork with a metal frame able to confine the soil macroblock. Furthermore, the roof was constructed over a perimeter timber beam (10x10 cm) at finished walls level (1.90 m) supporting two 45° masonry parapets (t= 17 cm including plaster at both faces) of fired-clay bricks and cement-sand mortar (Fig. 8(c)).

The perimeter beam also serves as a spandrel for the door and windows to distribute the roof weight to the

supporting walls.

The walls and triangular parapets were plastered (t= 1.5 cm) with a stabilized fine soil mix with a 3% of Portland cement. Each parapet has an intermediate support made of the same material with a rectangular shape of 30x30x50 cm. The triangular light roof system with final wings of 60 cm was constructed with a timber joist mesh (60x50 cm) and total length of 2.20 m (transversal section of 4x8 cm) for fixing the sheeting. The channeled compressed cardboard sheeting (1.20x0.65 m) with an overlapping of 20 cm was fixed with nails and bottle caps (Fig. 8(c)) as the traditional



(a) Anchorage between walls and cover



(b) General view of the construction process of the compressed soil blocks and formwork



(c) Roof of compressed cardboard sheeting



(d) General view of the finished small house

Fig. 8 Construction of the rammed soil walls, light cover and general view of the finished house

technique in Mexico for the construction of adobe housing. Fig. 8(d) shows the finished auto-constructed rammed soil house under study. For more information regarding the construction process of this case study, the reader is referred to Ayala (2004); Preciado *et al.* (2017) and Preciado and Santos (2019).

5. Damage identification after 15 years in the self-build rammed soil house

Recently, in 2019, it has been 15 years since the construction of the earthen house and has suffered different damages due to the constant seismicity of the region (see Table 3), vandalism, aging, weather degradation, biological attack and lack of maintenance as observed in Fig. 9.

The house of Fig. 9 was constructed about one year and a half after the destructive Tecoman-Armeria EQ in 2003 ($M_w = 7.5$, $MMI = VII-VIII$), which caused strong damages and casualties in Colima City and neighbor towns including the Manzanillo port (see Table 2). The earthen house (see Fig. 9) has survived (2004-2019) different EQs ranging from $M_w = 5.5$ to 6.4 (see Table 3) induced by the surrounding complex seismic sources that were previously explained in Section 3. Since the finishing of the house in summer 2004, it was not developed any study on the house and it was until May 2016 when it was decided to analyze the involved damages due to the lack of maintenance and seismicity of the region. It was observed that the structure

Table 3 Overview of main EQs ($M_w \geq 5.5$) from 2003 to 2018 occurred near Colima City (SSN 2019)

Event	Date	Lat. N	Long. W	M_w	Depth km	Reference
1	06/29/2018	18.88°	105.27°	5.9	15.7	84 km SW from Cihuatlan
2	11/03/2017	18.71°	106.52°	5.6	16.2	214 km SW from Cihuatlan
3	06/07/2016	18.28°	105.31°	6.1	8.7	131 km SW from Cihuatlan
4	02/12/2015	19.16°	105.91°	5.5	15	142 km W from Cihuatlan
5	02/20/2013	18.50°	103.99°	5.6	3.2	46 km SW from Tecoman
6	09/23/2008	17.64°	105.61°	6.4	16	208 km SW from Manzanillo
7	11/19/2006	18.33°	104.36°	5.6	13	79 km SW from Armeria
8*	01/21/2003	18.63°	104.13°	7.6	9	46 km SW from Armeria

presented a strong damage by aging with the decay of plasters (see that the brick masonry became evident on parapets) due to the heavy rain and weathering, as well as damage of the cover system due to the house was used as a storehouse of scholar furniture and other waste (Fig. 9(a)). The damaged cardboard sheeting of the cover system allowed the entrance of raining water to the interior part of the house and caused damage to the timber elements including the perimetral beam and triangular masonry parapets. The perimetral timber beam is extremely decayed

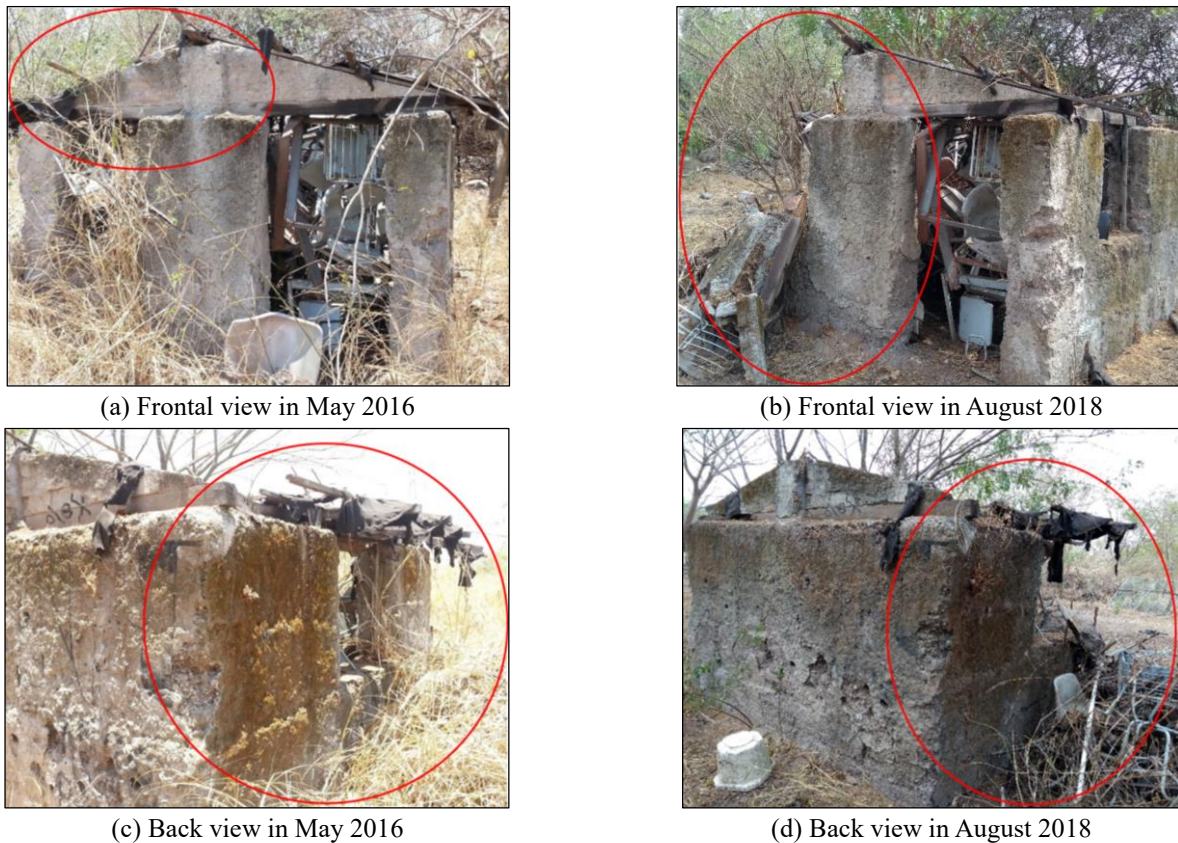


Fig. 9 Actual conservation state of the rammed soil house

and also the appearance of the rammed soil walls has changed due to moisture and aging. It was also observed induced moisture to supporting walls at the four façades as illustrated in Fig. 9(c). In May 2016, the supporting walls of the house remained without collapsed parts, just the presence of multiple cracks induced by raining degradation and the presence of biological attack (e.g., cavities generated by insects and invasive plants). In general terms, in the 2016 survey, the seismic performance of the house was considered as relatively satisfactory due to the reduced weight of the cover, great wall thickness and anchorage system between cover and corners of walls (Fig. 9(a) and 9(c)). In August 2018, another in-situ campaign was developed to analyze the decay degradation which considerably increased and it was surprising to observe that the right part of the frontal façade presented an important collapse as shown in Fig. 9b and d. The corner walls collapsed including a half part of the parapet and it was considered that the probable cause was the constant seismicity of the region. Therefore, it was developed an investigation of recent EQs occurred near Colima City. In Table 3 it is shown that after the technical visit developed in May 2016, three important EQs ranging from $M_w=5.6$ to 6.1 (i.e., 2016, 2017 and 2018) have occurred in the surroundings of Colima City.

6. Sampling extraction and uniaxial testing in existing walls

In late summer 2018, it was extracted several coarse

samples of approximately 25x25x25 cm from some walls including the collapsed ones with cutting tools (Fig. 10(a)) to investigate the impact of aging on the strength degradation of the existing rammed soil walls exposed to extreme weathering and zero-maintenance. The sampling extraction was difficult due to the presence of large stones inside the walls with average diameters ranging from 2.5-10 cm. The coarse samples were packaged (Fig. 10(b)) and transported to ITESO University in Guadalajara, Jalisco (180 km from Colima City) in order to be subjected under different investigations such as uniaxial compressive tests with a universal test machine (UTM) (Fig. 11(a)) and its correlation to the water content, materials composition and failure mechanisms under extreme loading. From the coarse wall samples (Fig. 10b), it was extracted more segments and were carved until reaching cubes with final average dimensions of 6.5x7.5x8.5 cm (Table 4) capped with a slight layer of gypsum (see Figs. 11(b) and 11(c)) for a uniform loading transmission with the UTM. The observed failure mechanisms in the extracted samples M1-M5 under uniaxial compression tests are shown in Fig. 12, where it is worth noting in all cases, the typical crushing behavior and a rapid propagation of vertical and semi-diagonal distribution of cracks (Fig. 12(a)-12(c)). Some of the samples only shown several vertical/diagonal cracks (Fig. 12(a)), other ones just a large vertical crack (Fig. 12(b)) and the rest, a combination of cracks (Fig. 12(c)). The stress-strain curves and envelope of the existing wall samples M1-M5 under uniaxial compression tests are illustrated in Fig. 13(a). It is worth noting that the five samples presented a



(a) Destructive sampling extraction



(b) Packaging for transportation

Fig. 10 Rammed soil walls sampling extraction and transportation



(a) Universal test machine



(b) Carved samples weighting



(c) Samples capping with gypsum

Fig. 11 M1-M5 samples of existing rammed soil walls for the destructive tests under compression



(a) Several vertical/diagonal cracks



(b) Vertical cracks



(c) Multiple vertical/diagonal cracks

Fig. 12 Observed failure mechanisms on existing samples of rammed soil walls M1-M5

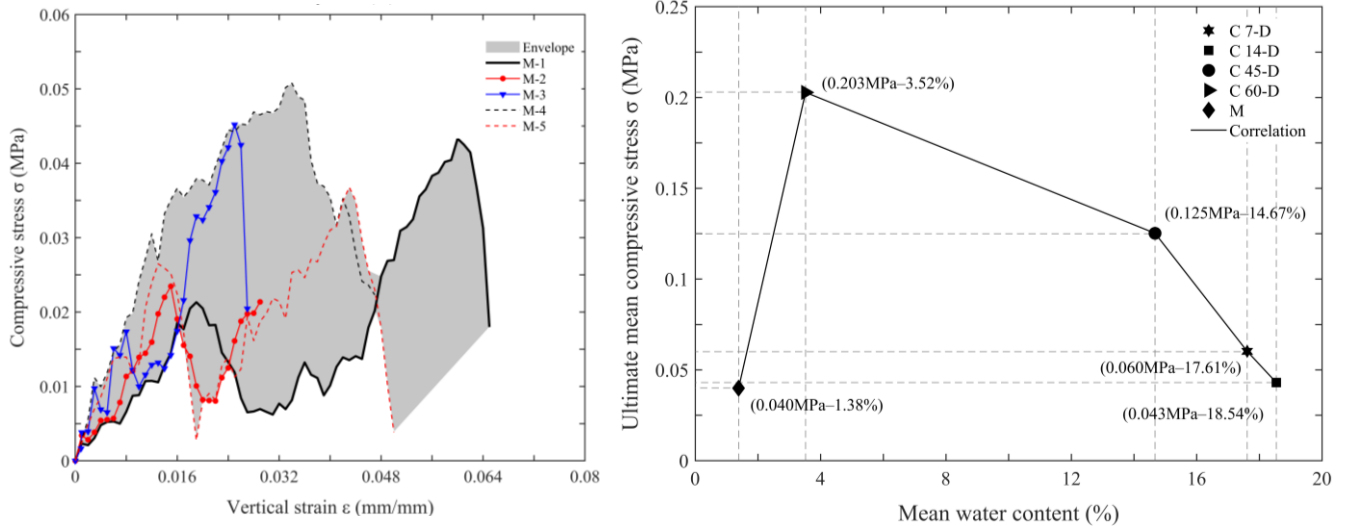
certain sawtooth behavior (see the formed peaks in Fig. 13(a)) due to the interlocking effect by the presence of gravel with a diameter higher than 2.5 cm (see Figs. 11(b), 11(c) and 12). This effect induces micro-cracks inside the samples and hard zones by the interaction of one segment of gravel with another, leading to either, an increasing of strength or its degradation.

The aforementioned interlocking may be the reason of increasing compressive stress in some specimens (e.g., M1 and M2) after a drastic drop in the stress-strain curves. Table 4 presents a summary of physical and mechanical properties of the existing samples M1-M5 under uniaxial compression in terms of elastic, plastic and post-peak

behavior. The samples presented a mean elastic compressive strength of 0.0120 MPa with an E modulus of 1.45 MPa and an ultimate compressive strength of about 0.040 MPa (0.408 kg/cm²).

Moreover, the samples M1-M5 shown at the day of testing a mean water content of 1.38% (see Table 4 and Fig. 13(b)). The observed mechanical properties are quite below the reported results of new compacted soil samples (Table 1).

It is worth noting that the results of this research regarding compressive strength after 15 years of degradation may be of contribution due to most of cases reported in literature are focused on new samples. Fig.



(a) Stress-strain curves of existing wall samples M1-M5 (b) Correlation between ultimate mean compressive strength and mean water content of existing samples M1-M5 and new soil cylinders C

Fig. 13 Summary of results of existing samples M1-M5 of rammed soil walls and new soil cylinders C at different ages under compression

Table 4 Summary of main physical and mechanical properties of the existing samples M1-M5 (15-year-old) under uniaxial compression

Cube	t mm	l mm	h mm	A mm ²	ω_f %	σ_{el} MPa	ϵ_{el} mm/mm	σ_u MPa	ϵ_u mm/mm	E MPa
M - 1	62.14	88.37	90.42	5491.00	1.65	0.0130	0.01412	0.0433	0.06000	0.92
M - 2	75.85	76.19	94.85	5778.25	1.25	0.0070	0.00662	0.0235	0.01500	1.06
M - 3	60.00	58.29	91.82	3497.11	1.24	0.0136	0.00874	0.0452	0.02500	1.55
M - 4	67.60	71.37	65.16	4824.61	1.30	0.0152	0.00659	0.0508	0.03400	2.31
M - 5	57.95	77.62	83.42	4497.69	1.44	0.0110	0.00790	0.0368	0.04300	1.40
Mean	64.71	74.37	85.13	4817.73	1.38	0.0120	0.00880	0.0399	0.03540	1.45

t= thickness; l= length; h= height; A= area; ω_f = water content at test; σ_{el} = compressive stress at yielding; ϵ_{el} = elastic deformation; σ_u = ultimate compressive stress; ϵ_u = deformation at ultimate and E= elasticity modulus

13(b) illustrates the correlation between mean compressive strength and water content at ultimate conditions of the existing rammed soil wall samples (M1-M5) with the code M, as well as the results on new soil samples (cylinders) with the code C tested under compression at different ages (i.e., 7, 14, 45 and 60 days). Fig. 13(b) is explained more in detail with the obtained results for new soil samples C in Section 7. Regarding the shear strength of the existing rammed soil house, it was not possible to extract representative samples with enough size (e.g., 30x30 cm) to be transported and tested with the UTM machine due to the brittleness of this material. Hence, the obtained ultimate compressive strength (0.040 MPa) of the existing house (samples M1-M5) may serve as indicator of shear strength by considering an average of 15% (0.006 MPa). This percentage was determined according to the compressive/shear strength properties of rammed soil specimens reported in Table 1, e.g., Silva *et al.* (2014b) (12% of the compressive strength); Afanador-Garcia *et al.* (2013) (13%) and Meli (1998) (10-25%).

7. Uniaxial and shear testing of new soil cylinders and wallettes

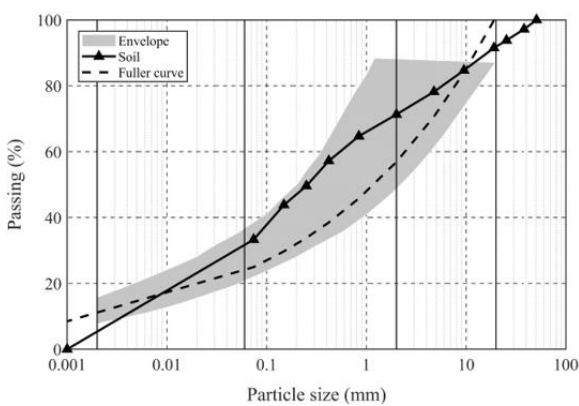
In order to compare the degraded uniaxial compressive strength of the existing rammed earth walls, new soil specimens were fabricated. For achieving the last, it was extracted different soil samples from the same construction site where the self-constructed house is located (Fig. 14(a)) and fabricated in laboratory 12 cylinders of h= 20 cm and d= 10 cm (see Fig. 14(b)).

The soil mix presented a granulometry of 33.34% of fines (clay and silt), 44.84% of sand and 21.82% of gravel with a density of 1809 kg/m³ (a dried density of 1136 kg/m³). These physical soil properties are in agreement with the properties reported in literature for good quality soils for rammed earth structures (see Table 1). Moreover, these properties are also similar to the used earth in the construction of the house, due to the soil was extracted from the same site. In addition of the soil classification, it was subjected to a detailed sieving analysis (i.e., particle size distribution) to determine the quantitative properties of the

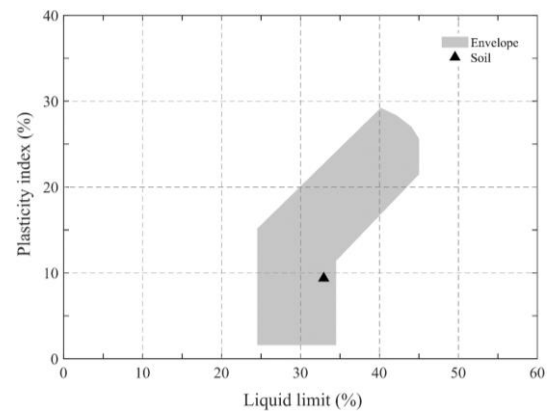


(a) Excavation at the back part of the house under study in summer 2018 (b) New soil specimens C for the uniaxial compressive tests

Fig. 14 Extracted soil samples and new specimens



(a) Fuller curve, envelope of suitable soils proposed by Houben and Guillaud (2008) and soil under study



(b) Liquid limit and plasticity index of the soil under study

Fig. 15 Quantitative properties of the extracted soil samples based on granulometry tests

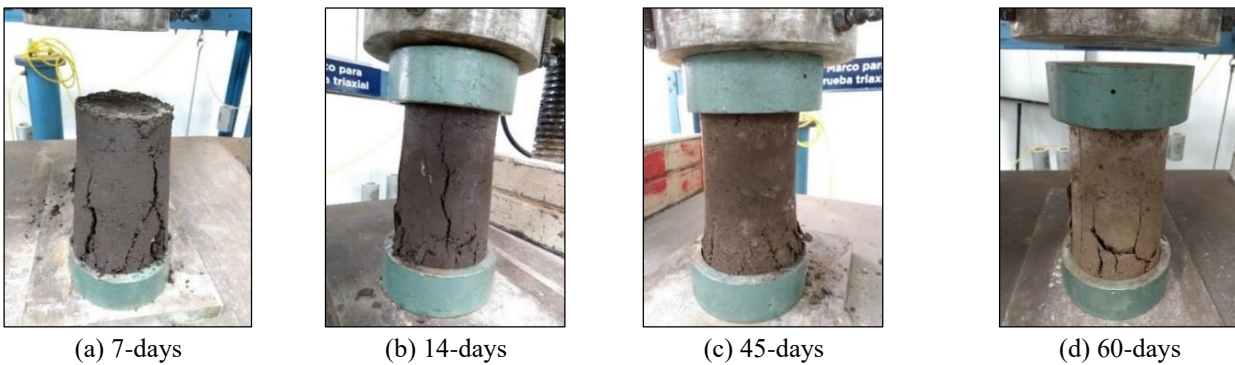


Fig. 16 Observed failure modes under compression in new soil specimens C at different ages

new extracted samples. This analysis allowed to determine the Fuller curve as shown in Fig. 15(a).

This methodology is used in highway engineering in the design of pavements. Moreover, if the soil is located close enough of the Fuller curve or inside the envelope of suitable soils for rammed earth proposed by Houben and Guillaud (2008), then it might be considered as a soil with acceptable characteristics. It is worth noting in Fig. 15(a), that the soil under study fits well inside the envelope, even when it is slightly different than the Fuller curve. Another great advantage of this strategy, is that it allows the possibility of

correcting the soil by the addition of fines, sand or gravel in terms of percentage with the sieving methodology. Moreover, with the use of the Atterberg limits, it is possible to determine other important quantitative soil properties such as the consistency or plasticity limits: the soil under study exhibited a liquid limit (LL) of 32.94%, a plastic limit (PL) of 23.56% and a plasticity index (PI) of 9.38% (LL-PL) (see the black triangle in Fig. 15(b)). The PI of 9.38% is representative of soils with a medium plasticity (7-17%). These soil properties are also in agreement with the reported limits and indexes in the relevant literature

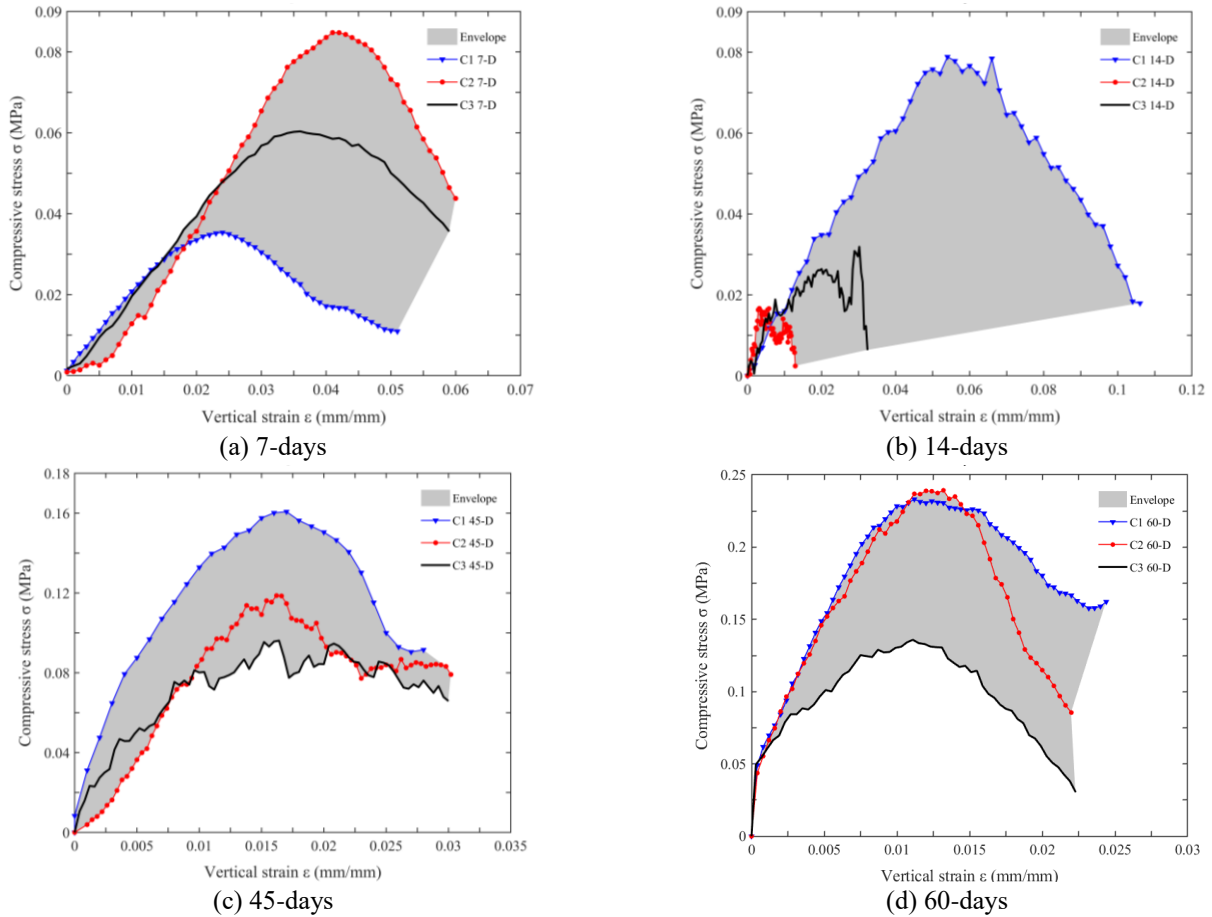
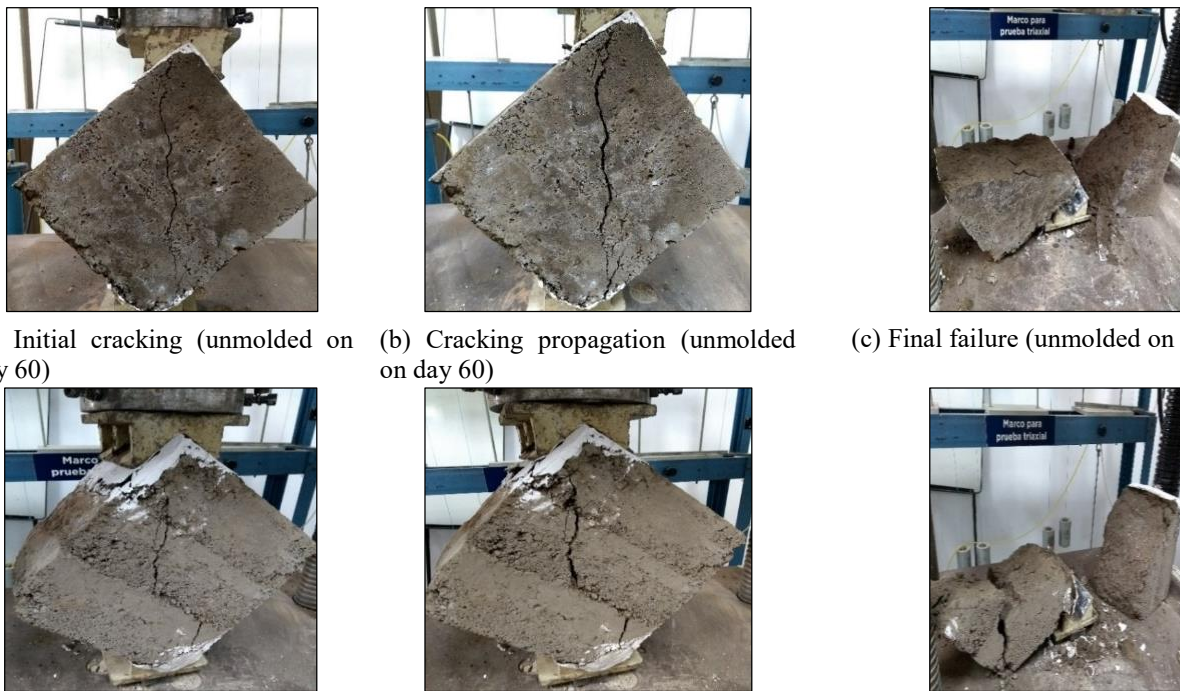


Fig. 17 Stress-strain curves of the new specimens *C* under compression at different ages



(a) Initial cracking (unmolded on day 60) (b) Cracking propagation (unmolded on day 60) (c) Final failure (unmolded on day 60)

(d) Initial stepped cracking (unmolded on day two) (e) Final cracking (unmolded on day two) (f) Ultimate failure (unmolded on day two)

Fig. 18 Observed failure modes under diagonal shear on new compressed soil wallettes unmolded at different stages and variations in water content %

Table 5 Summary of physical/mechanical properties of the new soil specimens under uniaxial compression

Cylinder Age	d mm	h mm	A mm ²	ω_f %	σ_{el} MPa	ε_{el} mm/mm	σ_u MPa	ε_u mm/mm	E MPa
C1 - 7D	99.91	192.60	7839.90	21.54	0.0106	0.00472	0.0353	0.02400	2.25
C2 - 7D	100.31	194.08	7902.80	17.14	0.0254	0.01586	0.0848	0.04100	1.60
C3 - 7D	100.40	199.27	7916.90	14.14	0.0181	0.00947	0.0604	0.03600	1.91
Mean 7D	100.21	195.32	7886.53	17.61	0.0180	0.0100	0.0602	0.0337	1.92
C1 - 14D	97.95	198.48	7535.30	17.77	0.0237	0.01315	0.0789	0.05400	1.80
C2 - 14D	98.92	192.79	7685.30	21.14	0.0050	0.00166	0.0166	0.00320	3.01
C3 - 14D	98.32	196.69	7592.30	16.71	0.0096	0.00411	0.0319	0.03020	2.33
Mean 14D	98.40	195.99	7604.3	18.54	0.0127	0.0063	0.0425	0.0291	2.38
C1 - 45D	99.06	196.75	7707.00	14.30	0.0482	0.00204	0.1607	0.01700	23.62
C2 - 45D	98.96	196.60	7691.00	15.41	0.0356	0.00493	0.1187	0.01620	7.22
C3 - 45D	98.34	193.20	7595.00	14.29	0.0288	0.00222	0.0961	0.01640	12.99
Mean 45D	98.79	195.52	7664.33	14.67	0.0376	0.0031	0.1252	0.0165	14.61
C1 - 60D	100.24	197.28	7891.70	1.58	0.0699	0.00121	0.2331	0.01120	57.87
C2 - 60D	98.03	197.64	7547.60	4.02	0.0718	0.00146	0.2393	0.01320	49.22
C3 - 60D	98.43	193.54	7609.30	4.96	0.0408	0.00025	0.1359	0.01110	165.52
Mean 60D	98.90	196.15	7682.87	3.52	0.0608	0.0010	0.2028	0.0118	90.87

d= diameter; h= height; A= area; ω_f = water content at test; σ_{el} = compressive stress at yielding; ε_{el} = elastic deformation; σ_u = ultimate compressive stress; ε_u = deformation at ultimate and E= elasticity modulus

Table 6 Summary of physical/mechanical properties of the two wallettes W1 and W2 under diagonal shear

Wallette	Unmolded	l mm	t mm	h mm	D mm	ω_f %	τ_u MPa	ε_u mm/mm	G_o MPa
W1-60D	on day 60	274.74	197.14	301.63	401.67	11.24	0.0176	0.0057	3.10
W2-60D	on day two	269.71	198.17	304.46	386.67	1.51	0.0605	0.0160	3.78
Mean		272.23	197.66	303.05	394.17	6.38	0.0391	0.0109	3.44

l= length; t= thickness; h= height; D= diagonal length; ω_f = water content at test; τ_u = ultimate shear stress; ε_u = deformation at ultimate and G_o = shear modulus

mentioned in the introductory sections of this research paper, as well as the envelope of suitable soils for rammed earth proposed by Houben and Guillaud (2008). In order to compare the plasticity properties of the soil in qualitative terms, it was developed the dropping ball test with an approximated water content of 18%. The samples presented a good plasticity without substantial cracks. Furthermore, the cylinders were filled up in three layers and compacted with a rammer until reaching a visual compaction as the artisanal technique (Fig. 14(b)). The new soil specimens were not capped, instead, it was used neoprene retainers (Fig. 16) to be tested with the UTM at different ages. The failure modes of the new soil samples *C* under compression are shown in Fig. 16. It is worth noting that the level of moisture evidently decreases with age. The correlation between water content and strength is also another relevant contribution of this paper (see Table 5 and Figs. 13(b), 16 and 17). The 7-days samples (moisture 17.61%) (Fig. 16(a)) mainly presented several vertical cracks ending with a semi-diagonal distribution, and the 14-days shown (moisture 18.54%) (Fig. 16(b)) a similar failure but with a combination of vertical cracks and bottom crushing. The 45-days (moisture 14.67%) (Fig. 16(c)) samples exhibited a

failure governed by bottom crushing and the 60-days (moisture 3.52%) (Fig. 16(d)) samples the formation of circular delamination and bottom crushing.

Fig. 17 illustrates the stress-strain curves of all samples under uniaxial compression and Table 5 the summary of physical and mechanical properties. The stress-strain curves of 7-days (Fig. 17(a)) and 14-days (Fig. 17(b)) samples presented a similar mean compressive strength (0.043-0.060 MPa). The strength increasing was observed in the 45-days specimens (Fig. 17(c)) with a mean ultimate stress of approximately two times higher than the observed in the 7-14-days ones (0.125 MPa). Furthermore, the 60-days samples (Fig. 17(d)) presented a mean compressive strength (0.203 MPa) of about 1.6 times higher than the 45-days ones, and in average, four times higher than the 7 and 14-days samples. The summary of physical and mechanical properties of the new soil specimens under uniaxial compression is shown in Table 5. The correlation between compressive strength and water content of the existing 15-year-old samples M1-M5 and the new soil cylinders *C* is illustrated in Fig. 13(b). It is worth noting that the 15-year-old samples presented an approximated mean compressive strength (0.040 MPa, 1.38% moisture) to that of the

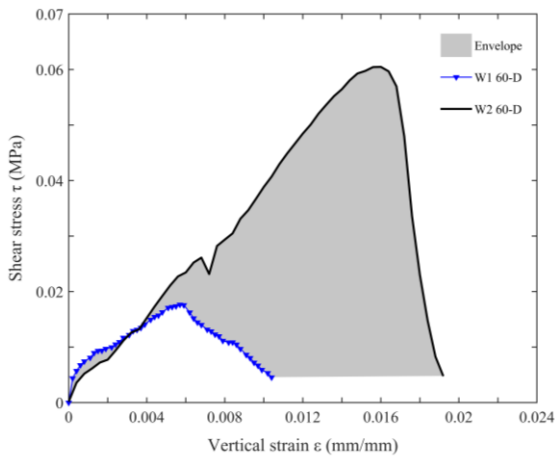


Fig. 19 Stress-strain curves of the two wallettes under diagonal shear (W1 unmolded on day 60 and W2 unmolded on day two)

exhibited by the 7-14-days samples (0.043-0.060 MPa, 17.61-18.54% moisture), but with a great difference regarding water content percentage. Moreover, the specimens tested at 60 days approximately presented 2.5 times more water content than the measured in the 15-year-old samples, but a substantial increasing in the mean ultimate strength (0.203 MPa, 3.52% moisture) of about 508% (five times higher).

Moreover, two wallettes W1 and W2 (272x303x198 mm) (Fig. 18 and Table 6) were fabricated with the extracted soil to be tested under diagonal compression in laboratory with the UTM. Besides of evaluating the shear strength and failure modes, both wallettes were fabricated considering a different number of compacted layers and a variable water content at the day of testing (i.e., 60-days). Table 6 presents a summary of physical/mechanical properties of the wallettes under diagonal shear. The first wallette (Fig. 18(a)) was compacted in two layers and unmolded until the testing day. This wallette presents a different composition of layers and moisture content (11.24%) (Table 6) if compared to the one shown in Fig. 18d (i.e., three layers and a water content of 1.51%) which was unmolded on day two. The observed shear failure modes on the two wallettes are also different (Fig. 18). The two-layers wallette (Fig. 18a) with more moisture presented the rapid formation of a diagonal crack (Fig. 18(b)) which ended with a final failure by separation in two parts (Fig. 18(c)). Conversely, the three-layers wallette with much less moisture (Fig. 18(d)) presented a different damage propagation by stepped cracking (Fig. 18(e)) and a final failure in three parts (Fig. 18(f)). The difference in the observed cracking propagation and failure mechanisms was also observed in the stress-strain behavior of both wallettes W1 and W2 (Fig. 19). The wallette W2 with a reduced moisture content (1.51%) shown almost 3.5 times more compressive strength (0.0605 MPa) and deformation at ultimate capacity (0.016 mm/mm) than wallette W1 (0.0176 MPa, 0.005 mm/mm and 11.24% of moisture). Regarding the comparative of mean shear (0.0391 MPa) and compressive strength of new samples tested at 60 days

(0.2028 MPa) (see Tables 5 and 6), it is worth noting that the mean shear stress is of about the 19% of the mean compressive strength. Analyzing the reported values in literature of Table 1, it is observed that there is a range of values of shear stresses between 10-15% of the compressive strength (e.g., Meli 1998 (10-15%), Afanador-Garcia *et al.* 2013 (13%), Silva *et al.* 2014b (12%)). However, more tests are needed to verify the observed behavior regarding the number of layers on the failure mechanisms and water content under shear stresses. It is proposed as a further work to construct at least three more samples of both wallettes, with two and three layers and different moisture content to validate the aforementioned behavior and failure.

Regarding the correlation of compressive strength with the moisture content (see Figs. 13 and 17) it was observed that the lower the moisture content, the higher the compressive strength. This is only valid for new rammed soil structures (1-5 years). This is not valid in the case of the uniaxial compressive testing on the 15-year-old samples, even when the moisture content is very low (e.g., 1.38%), due to the fact that the compressive strength is substantially affected by aging, micro-cracking, seismic damages, moisture propagation and biological attack (see Figs. 13 and 17). The moisture-compressive strength relationship also has an impact on the shear strength of new samples, and the number of layers on the failure mode through stepped cracking and may also contribute to a more energy dissipation as observed by other researchers in stone and brick masonry walls under lateral loading (e.g., Mistler 2006, Nateghi and Alemi 2008, Preciado and Sperbeck 2019).

8. Conclusions

Earthen structures have an excellent bioclimatic behavior and are sustainable construction systems, but they are earthquake prone structures with a poor performance and brittle failure mechanisms even against reduced lateral loading due to its low shear strength and nonlinear behavior. Colima, Mexico is under a very high seismic hazard due to its proximity to very active seismic zones with complex behavior which are responsible of causing strong damages/collapses on buildings and multiple casualties in past decades. In order to investigate the edification process and involved costs against conventional materials, a full-scale rammed soil house was constructed in 2004. Moreover, in 2016-2019, it became of relevance to take the opportunity to study its seismic performance, durability, degradation by aging and weathering with zero-maintenance. The 15-year-old rammed soil house presented huge advantages in terms of costs and sustainable benefits if compared to conventional houses of fired-clay brick masonry, but, conversely, the main drawback of rammed soil and adobe is the extreme needed effort to construct a small house, the lack of structural integrity and decay. In 2004, the water content and soil quality were determined by qualitative procedures. From 2004 to 2016 the house presented a relatively good seismic behavior against events with magnitudes ranging from 5.6 to 6.4 M_w . It was

observed a larger impact regarding the cover system, which was damaged by its use as a storage room and allowed the entrance of raining water and contributed in the fast deterioration of walls and the decay of timber elements, triangular parapets and plasters. The zero-maintenance increased the moisture propagation on walls and cover, as well as by the presence of biological attack and constant seismicity of the region.

In 2018 it was observed a partial collapse of one of the frontal walls may be due to seismic activity ranging from 5.6 to 6.1 M_w (i.e., 2016, 2017 and 2018), but there is no evidence of damage in other vulnerable housing in the surroundings. Several coarse samples were extracted from the collapsed wall and carved in laboratory in order to be analyzed under uniaxial compression and to study its correlation with the water content. The existing samples shown a reduced mean compressive strength (0.040 MPa) and a mean water content of about 1.38%. This low resistance is related to the material degradation by micro-cracks, moisture and biological attack. Taking into account these results, it is estimated that the existing house located in a tropical weather (average yearly temperature of 25°) has approximately a remaining 20% of compressive strength with a degradation of about 5.4% (0.0109 MPa) per year (considering a time frame of 15 years) if compared to the new soil samples (0.2028 MPa, 3.52% of moisture). This correlation between moisture and compressive strength degradation was compared with the study of about 20 cylinders of new soil samples from the same construction site and compared against the extracted samples from the 15-year-old house. At 7-14 days, the specimens presented a similar compressive strength (0.043-0.060) than the degraded 15-years ones (0.040 MPa, moisture= 1.38%), but with a very different water content (17.61-18.54%). Conversely, the 60-days samples (moisture%= 3.52) shown almost five times more compressive strength (0.203 MPa) if compared to the existing 15-year-old house samples (0.040 MPa, moisture%= 1.38) for a relatively similar water content. However, the observed higher compressive strength on the 60-days specimens (0.203 MPa, moisture%= 3.52) is reduced if compared to conventional brick masonry (1.5-2 MPa). In new rammed soil houses, the lower the water content (extending the 60 days), the higher the compressive strength. This correlation is only valid for new rammed soil walls, due to the fact that in existing aged houses the degradation per year plays an important role. The studied wallettes with different layers and water content under diagonal compression shown that the strength and failure modes are also influenced by the moisture content and by the number of layers. The observed shear failure mechanisms on the two wallettes are also different. The wallettes presented a mean shear stress of about the 19% of the mean compressive strength. It was not possible to obtain the shear strength of the existing rammed soil house due to the lack of extracted representative samples by the brittleness of this material. Thus, the obtained compressive strength (0.040 MPa) of the existing house may serve as indicator of shear strength by considering an average of 15%, resulting in 0.006 MPa.

The authors of this paper recommend 60-days as the

optimal time for rammed soil specimens (i.e., cylinders, cubes and wallettes) to reach their maximum compressive/shear strength in tropical weathers. However, more detailed investigations are suggested to understand/improve this brittle material to continue using for housing (or for reinforcing existing ones) against conventional materials (e.g., RC, fired-clay brick masonry, etc.). Moreover, it is recommended as a further research to test a larger number of rammed soil wallettes with different layers under diagonal compression to corroborate the observed stepped cracking and its contribution in a more ductile failure mode. Earthen houses such as adobe and rammed soil constructions are made of sustainable materials which are worth continuing investigating due to its relative construction simplicity, low-cost, materials availability and remarkable bioclimatic properties.

Acknowledgments

The first author of this paper would like to thank to his father Adolfo Preciado Ramirez for his fruitful comments and suggestions during the construction process of the rammed soil house in 2004 and by his help in the in-situ sampling extraction last summer 2018. Special thanks to the engineers of Labconstru Maza S.A. de C.V. for their collaboration in the soil characterization and mechanics as well as for the laboratory colleagues at ITESO University for their support with the UTM tests.

References

- Adam, E.A. and Jones P.J. (1995), "Thermophysical properties of stabilized soil building blocks", *Build. Environ.*, **30**(2), 245-253. [https://doi.org/10.1016/0360-1323\(94\)00041-P](https://doi.org/10.1016/0360-1323(94)00041-P).
- Afanador-Garcia, N., Carrascal-Delgado, M. and Bayona-Chinchilla, M. (2013), "Experimentación, comportamiento y modelación de la tapia pisada.", *Revista Facultad de Ingeniería* **22**(35), 47-59. <https://doi.org/10.19053/01211129.2514>.
- Ayala, K. (2004), "Costos de cimbra deslizable para compactar muros de tierra compactada", B.A. Thesis, Instituto Tecnológico de Colima, Colima, Mexico.
- Bahar, R., Benazzoung, M. and Kenai, S. (2004), "Performance of compacted cement stabilized soil", *Cement Concrete Comp.*, **26**(7), 811-820. <https://doi.org/10.1016/j.cemconcomp.2004.01.003>
- Bakir, N., Abbeche, K. and Panczer, G. (2017), "Experimental study of the effect of the glass fibers on reducing collapse of a collapsible soil", *Geomech. Eng.*, **12**(1), 71-83. <https://doi.org/10.12989/gae.2017.12.1.071>.
- Bandy, W., Mortera-Gutierrez, C., Urrutia-Fucugauchi, J. and Hilde, T.W.C. (1995), "The subducted Rivera-Cocos plate boundary: Where is it, what is it, and what is its relationship to the Colima rift?", *Geophys. Res. Lett.*, **22**(22), 3075-3078. <https://doi.org/10.1029/95GL03055>.
- Bui, Q.B., Morel, J.C., Venkatarama-Reddy, B.V. and Ghayad, W. (2009), "Durability of rammed earth walls exposed for 20 years to natural weathering", *Build. Environ.*, **44**(5), 912-919. <https://doi.org/10.1016/j.buildenv.2008.07.001>.
- Burroughs, S. (2008), "Soil property criteria for rammed earth stabilization", *J. Mater. Civ. Eng.*, **20**(3), 264-273. [https://doi.org/10.1061/\(ASCE\)0899-1561\(2008\)20:3\(264\)](https://doi.org/10.1061/(ASCE)0899-1561(2008)20:3(264)).
- Caporale, A., Parisi, F., Asprone, D., Luciano, R. and Prota, A.

- (2015), "Comparative micromechanical assessment of adobe and clay brick masonry assemblages based on experimental data sets", *Compos. Struct.*, **120**, 208-220.
<https://doi.org/10.1016/j.compstruct.2014.09.046>.
- Chavez, M., Garcia, S., Cabrera, E., Ashworth, M., Perea, N., Salazar, A., Chavez, E., Saborio-Ulloa, J. and Saborio-Ortega, J. (2014), "Site effects and peak ground accelerations observed in Guadalajara, Mexico, for the 9 October 1995 Mw 8 Colima-Jalisco, Earthquake", *B. Seismol. Soc. Am.*, **104**(5), 2430-2455.
<http://doi.org/10.1785/0120130144>.
- Dayton, L. (1991), "Saving mud monuments", *New Sci.*, **130**, 38-42.
- De Morsier, Y. (2011), *Our Experience with Rammed Earth: A Manual for Rammed Earth Building*, www.desertcreekhouse.com.au.
- DeMets, C. and Traylen, S. (2000), "Motion of the Rivera plate since 10 Ma relative to the Pacific and North American plates and the mantle", *Tectonophysics*, **318**(1-4), 119-159.
[https://doi.org/10.1016/S0040-1951\(99\)00309-1](https://doi.org/10.1016/S0040-1951(99)00309-1).
- Easton, D. (1996), *The Rammed Earth House*, Chelsea Green Publications Company, Vermont, U.S.A.
- Flores-Estrella, H., Ramirez-Gaytan, A., Sarnecki, P., Preciado, A., Lazcano, S., Alcantara, L. and Korn, M. (2018), "Vs30 maps and fundamental periods in Guadalajara, Jalisco, Mexico, obtained from seismic noise analysis", *Proceedings of the 36th General Assembly of the European Seismological Commission*. Valletta, Malta, September.
- Gupta, D. and Kumar, A. (2017), "Stabilized soil incorporating combinations of rice husk ash, pond ash and cement", *Geomech. Eng.*, **12**(1), 85-109.
<https://doi.org/10.12989/gae.2017.12.1.085>.
- Hall, M., and Djerbib, Y. (2004), "Rammed earth sample production: Context, recommendations and consistency", *Constr. Build. Mater.*, **18**(4), 281-286.
<https://doi.org/10.1016/j.conbuildmat.2003.11.001>.
- Hall, M.R. (2007), "Assessing the environmental performance of stabilised rammed earth walls using a climatic simulation chamber", *Build. Environ.*, **42**(1), 139-145.
<https://doi.org/10.1016/j.buildenv.2005.08.017>.
- Houben, H. and Guillaud H. (2008), *Earth Construction, A comprehensive Guide*, Third edition, CRATerre – EAG, Intermediate Technology Publication, London, U.K.
- Islam, M.S. (2002), "Research on earthquake resistant reinforcement of adobe structures", Ph.D Thesis, Saitama University, Saitama, Japan.
- Islam, M.S. and Watanabe, H. (2004), "FEM simulation of seismic behaviour of adobe structures", *Proceedings of the 13th World Conference on Earthquake Engineering*. Vancouver, B.C., Canada, August.
- Jaquin, P.A., Augarde, C.E. and Gerrard, C.M. (2006), "Analysis of historic rammed earth construction", *Proceedings of the International Conference on Structural Analysis of Historical Constructions (SAHC)*, New Delhi, India, November.
- Keable, J. (1994), "Rammed Earth Standards", ODA Final Project Report R 4864C, London, U.K.
- Keable, J. (1996), *Rammed Earth Structures*, A Code of Practice, Intermediate Technology Publications, London, U.K.
- Khadka, B. and Shakya, M. (2016), "Comparative compressive strength of stabilized and un-stabilized rammed earth", *Mater. Struct.*, **49**(9), 3945-3955.
<https://doi.org/10.1617/s11527-015-0765-5>
- Kim, Y., Dang, M.Q., Do, T.M. and Lee, J.K. (2018), "Soil stabilization by ground bottom ash and red mud", *Geomech. Eng.*, **16**(1), 105-112.
<https://doi.org/10.12989/gae.2018.16.1.105>.
- Lourenço, P.B. and Pina-Henriques, J. (2006), "Validation of analytical and continuum numerical methods for estimating the compressive strength of masonry", *Comput. Struct.*, **84**(29-30), 1977-1989. <https://doi.org/10.1016/j.compstruc.2006.08.009>.
- Maniatidis, V. and Walker, P. (2003), *A Review of Rammed Earth Construction*, in *DTi Partners in Innovation Project: Developing Rammed Earth for UK housing*, U.K.
- Maniatidis, V. and Walker, P. (2008), "Structural capacity of rammed earth in compression", *J. Mater. Civ. Eng.*, **20**(3), 230-238. [https://doi.org/10.1061/\(ASCE\)0899-1561\(2008\)20:3\(230\)](https://doi.org/10.1061/(ASCE)0899-1561(2008)20:3(230)).
- Meli, R. (2008), *Structural Engineering of the Historical Buildings*, Civil Engineers Association (ICA) Foundation, A.C., Mexico City, Mexico (in Spanish).
- Milani, G. (2011a), "Simple lower bound limit analysis homogenization model for in- and out-of-plane loaded masonry walls", *Constr. Build. Mater.*, **25**(12), 4426-4443.
<https://doi.org/10.1016/j.conbuildmat.2011.01.012>.
- Milani, G. (2011b), "Simple homogenization model for the non-linear analysis of in-plane loaded masonry walls", *Comput. Struct.*, **89**(17-18), 1586-1601.
<https://doi.org/10.1016/j.compstruc.2011.05.004>.
- Mistler, M. (2006), "Deformation-based seismic measure concept for masonry constructions", Ph.D. Thesis, University of Aachen, Aachen, Germany (in German).
- Morel, J.C., Mesbah, A., Oggero, M. and Walker, P. (2001), "Building houses with local materials: Means to drastically reduce the environmental impact of construction", *Build. Environ.*, **36**(10), 1119-1126.
[http://doi.org/10.1016/S0360-1323\(00\)00054-8](http://doi.org/10.1016/S0360-1323(00)00054-8).
- Morris, H., Walker, R. and Drupsteen, T. (2010), "Observations of the performance of earth buildings following the September 2010 Darfield earthquake", *B. N.Z. Soc. Earthq. Eng.*, **43**(4), 393-403. <https://doi.org/10.5459/bnzsee.43.4.393-403>.
- Nateghi, F. and Alemi, F. (2008), "Experimental study of seismic behaviour of typical Iranian URM brick walls", *Proceedings of the 14th World Conference on Earthquake Engineering (WCEE)*. Beijing, China, October.
- Preciado, A. and Santos, J.C. (2019), "Rammed earth sustainability and durability in seismic areas as a building material", *Proceedings of the International Conference on Sustainability in the Built Environment for Climate Change Mitigation (SBE19)*, Thessaloniki, Greece, October.
- Preciado, A. and Sperbeck, S.T. (2019), "Failure analysis and performance of compact and slender carved stone walls under compression and seismic loading by the FEM approach", *Eng. Fail. Anal.*, **96**, 508-524.
<https://doi.org/10.1016/j.engfailanal.2018.11.009>.
- Preciado, A., Ayala, K., Torres, S., Villarreal, K., Gutiérrez, N., Flores, A. and Hernández, V. (2017), "Performance of a self-build rammed earth house in a high seismic zone of Mexico", *Proceedings of the 3rd International Conference on Protection of Historical Constructions (PROHITECH)*, Lisbon, Portugal, July.
- Preciado, A., Ramirez-Gaytan, A., Salido-Ruiz, R.A., Caro-Becerra, J.L. and Lujan-Godínez, R. (2015b), "Earthquake risk assessment methods of unreinforced masonry structures: Hazard and vulnerability", *Earthq. Struct.*, **9**(4), 719-733.
<https://doi.org/10.12989/eas.2015.9.4.719>.
- Preciado, A., Ramirez-Gaytan, A., Santos, J.C. and Rodríguez, O. (2020b), "Seismic vulnerability assessment and reduction at a territorial scale on masonry and adobe housing by rapid vulnerability indicators: The case of Tlajomulco, Mexico", *Int. J. Disaster Risk Reduct.*, **44**, 101425.
<https://doi.org/10.1016/j.ijdr.2019.101425>
- Preciado, A., Rodríguez, O., Caro-Becerra, J.L. and Lujan-Godínez, R. (2015a), "Escenarios de daño sísmico a escala territorial en mampostería no reforzada en Tlajomulco, Jalisco", *Proceedings of the Memorias del XX Congreso Nacional de Ingeniería Sísmica, Sociedad Mexicana de Ingeniería Sísmica*

- (SMIS), Acapulco, México, November (in Spanish).
- Preciado, A., Santos, J.C., Silva, C., Ramírez-Gaytan, A. and Falcon, J.M. (2020a), “Seismic damage and retrofitting identification in unreinforced masonry Churches and bell towers by the September 19, 2017 (Mw= 7.1) Puebla-Morelos Earthquake”, *Eng. Fail. Anal.*, **118**, 104924. <https://doi.org/10.1016/j.engfailanal.2020.104924>.
- Ruiz-Garcia, J. (2017), “Observations from the September 19, 2017 (Mw=7.1) Puebla-Morelos Earthquake in Mexico City”, Earthquake Engineering Research Institute (EERI), State University of Michoacan, U.S.A.
- Silva, R.A., Jaquin, P., Oliveira, D.V., Miranda, T., Schueremans, L. and Cristelo, N. (2014a), *Conservation and New Construction Solutions in Rammed Earth*, in *Structural Rehabilitation of Ancient Buildings*, Springer-Verlag, Berlin, Germany.
- Silva, R.A., Oliveira, D.V., Schueremans, L., Miranda, T. and Machado, J. (2014b), “Shear behaviour of rammed earth walls repaired by means of grouting”, *Proceedings of the 9th International Masonry Conference*, Guimarães, Portugal, July.
- SMIS and EERI (2006), “Preliminary observations on the Tecoman, Colima, Mexico, earthquake of January 21st, 2003 (in Spanish): Especial earthquake report (learning from earthquakes)”, Mexican Society of Seismic Engineering (SMIS) and the Earthquake Engineering Research Institute (EERI), Mexico City, Mexico.
- SSN (2019), Servicio Sismológico Nacional: catálogo de sismos; Universidad Nacional Autónoma de México, México. www.ssn.unam.mx.
- Standards Australia (2002), *The Australian Earth Building Handbook*, Standards Australia, Sydney, Australia.
- Standards New Zealand (1998), NZS 4298: 1998 Materials and workmanship for earth buildings—incorporating amendment No. 1; Standards New Zealand, Wellington, New Zealand.
- Taghiloha, L. (2013), “Using rammed earth mixed with recycled aggregate as a construction material”, M.E. Thesis, Universitat Politècnica de Catalunya, Barcelona, Spain.
- Varum, H., Tarque, N., Silveira, D., Camata, G., Lobo, B., Blondet, M., Figueiredo, A., Muhammad, M.R., Oliveira, C. and Costa, A. (2014), *Structural Behaviour and Retrofitting of Adobe Masonry Buildings*, in *Structural Rehabilitation of Old Buildings, Building Pathology and Rehabilitation*, Springer-Verlag, Berlin, Germany.
- Walker, P. (2005), *Rammed Earth: Design and Construction Guidelines*, BRE Bookshop, Watford, U.K.
- Yilmaz, Y., Eun, J. and Goren, A. (2018), “Individual and combined effect of Portland cement and chemical agents on unconfined compressive strength for high plasticity clayey soils”, *Geomech. Eng.*, **16**(4), 375-384. <https://doi.org/10.12989/gae.2018.16.4.375>.
- Zobin, V.M. and Pizano-Silva, J.A. (2007), “Macroseismic study of the Mw 7.5 21 January 2003 Colima, México, across-trench Earthquake”, *B. Seismol. Soc. Am.*, **97**(4), 1221-1232. <http://doi.org/10.1785/0120060080>.
- Zobin, V.M., Ventura-Ramirez, J.F., Gutierrez-Andrade, C.L., Hernandez-Cruz, L. and Santibañez-Ibañez, S. (2006), “The Mw 7.4 Colima, Mexico, Earthquake of 21 January 2003: The observed damage matrix in Colima City and its comparison with the damage probability matrix”, *Nat. Hazards*, **38**(3), 391-410. <https://doi.org/10.1007/s11069-005-2074-8>.